Dynamical properties of water-methanol solutions

Francesco Mallamace,[1,2,3] Carmelo Corsaro,[1,2] Domenico Mallamace,[4] Cirino Vasi,[2] Sebastiano Vasi,[1] and H. Eugene Stanley[3]
[1]*Dipartimento MIFT, Sezione di Fisica, Università di Messina, I-98166 Messina, Italy*
[2]*Consiglio Nazionale delle Ricerche-IPCF Messina, I-98158 Messina, Italy*
[3]*Center for Polymer Studies and Department of Physics, Boston University, Boston, Massachusetts 02215, USA*
[4]*Consorzio per lo Sviluppo dei Sistemi a Grande Interfase, Unità di Catania, I-95125 Catania, Italy*

(Received 10 November 2015; accepted 22 January 2016; published online 11 February 2016)

We study the relaxation times t_α in the water-methanol system. We examine new data and data from the literature in the large temperature range $163 < T < 335$ K obtained using different experimental techniques and focus on how t_α affects the hydrogen bond structure of the system and the hydrophobicity of the alcohol methyl group. We examine the relaxation times at a fixed temperature as a function of the water molar fraction X_W and observe two opposite behaviors in their curvature when the system moves from high to low T regimes. This behavior differs from that of an ideal solution in that it has excess values located at different molar fractions ($X_W = 0.5$ for high T and 0.75 in the deep supercooled regime). We analyze the data and find that above a crossover temperature $T \sim 223$ K, hydrophobicity plays a significant role and below it the water tetrahedral network dominates. This temperature is coincident with the fragile-to-strong dynamical crossover observed in confined water and supports the liquid-liquid phase transition hypothesis. At the same time, the reported data suggest that this crossover temperature (identified as the Widom line temperature) also depends on the alcohol concentration. © *2016 AIP Publishing LLC.* [http://dx.doi.org/10.1063/1.4941414]

I. INTRODUCTION

Understanding the unusual properties of water, which play an essential role in biological processes, is a topic of great interest in both science—including the fields of physics, chemistry, and biology—and technology. Water exhibits properties that are unusual and counterintuitive when compared with normal liquids. The behavior of a number of thermodynamic and transport properties in water, especially in the supercooled regime,[1,2] is anomalous. Below its melting point T_M, liquid water exhibits divergent-like behavior in its thermodynamic response functions. Another current water puzzle is its glass transition temperature.[3] The clustering behavior in the hydrogen-bond (HB) network is now commonly accepted to be the cause of these anomalous properties. When T decreases, the HBs cluster and form an open tetrahedrally coordinated HB network. When the T of the stable liquid phase is lowered, HB lifetime and cluster stability increase. This altered local structure, in principle, continues down to the amorphous region of the phase diagram where two glassy phases, characterized by different densities, have been observed.[4] The HB tetrahedrally coordinated network emerges because the oxygen atom in a water molecule has two hydrogen-donating sites, and the two hydrogens are single acceptors.

Glassy polymorphism is one of the most intriguing properties of water because the two amorphous phases have different densities. There is a first-order transition between high-density amorphous ice (HDA) and low-density amorphous ice (LDA) that occurs when the pressure and temperature are changed.[4,5] This suggests that liquid water may also be polymorphous,[3,6] i.e., a mixture of a low-density liquid (LDL) and a high-density liquid (HDL). The HDL predominates in the high T regime when the local tetrahedrally coordinated structure is not fully developed; whereas in the LDL, an open "ice-like" HB network is present. The anomalous behavior of water is caused by the "competition" between these two local liquid forms, and the HB clustering that occurs when the temperature is lowered into the supercooled state is behind the diverging behavior of the various liquid water thermal response and transport functions.

The water P–T phase diagram is rich, includes the liquid and the amorphous phases, and also ice in its many structural forms. At ambient pressure, metastable supercooled water is located between the melting temperature $T_M = 273$ K and the homogeneous nucleation temperature $T_H = 231$ K (the glass transition temperature being $T_g = 160$ K). The region between T_H and $T_X \sim 150$ K is not easily accessible experimentally in bulk liquid water and is referred to as "No-Man's Land". Crystallization within this No-Man's Land can be retarded somewhat by confining water within narrow nanoporous structures or mixing it with systems resistant to crystallization, e.g., salt or glycerol.[3] Studies of confined water[7–9] at ambient pressure have found that decreasing T greatly increases HB networking and HB lifetime, and that at $T_L \simeq 225$ K, there is a fragile-to-strong dynamic crossover (FSDC) where both LDL and HDL are observed.[7] This confirms the existence of liquid water polymorphism[6] and supports the liquid-liquid phase transition (LLPT) hypothesis.[10]

Water is considered as a prototype glass-forming material. Recent studies of confined water at ambient pressure have found anomalous dynamic properties inside the No-Man's Land including a density minimum at ≈200 K, an extreme in

 © 2016 AIP Publishing LLC

Reuse of AIP Publishing content is subject to the terms: https://publishing.aip.org/authors/rights-and-permissions. Downloaded to IP: 129.74.250.206 On: Fri, 19 Feb 2016 14:05:33

the thermal expansion coefficient $\partial \ln \rho/\partial T$ and specific heat $C_P(T)$,[7,8,11,12] and a FSDC[13–17] accompanied by the violation of the Stokes-Einstein relation (SER),[18] at and below the FSDC temperature. Glass-forming liquids are "strong" if their transport parameters exhibit an Arrhenius behavior. They are "fragile" if their transport parameters exhibit behavior that can be described by a Vogel-Fulcher-Tammann (VFT) relation. All of these phenomena occur at approximately the same temperature ($T_L = T_{\rm cross} \simeq 225$ K). The extrema in $\partial \ln \rho/\partial T$ and $C_P(T)$ provide, for the first time, evidence that the thermodynamical anomalies in water are not critical-point-like divergences.

Aqueous solutions of small amphiphilic molecules can thus be used as model systems to test water HB interactions and the resulting HB networks. The simplest amphiphilic molecule is methanol, CH_3OH, which consists of a single hydrophilic (OH) and a single hydrophobic (CH_3) group. Unlike water, methanol is a strong glass-forming liquid and exhibits an Arrhenius behavior ($\eta = \eta_0 \exp(E/k_BT)$) in the wide temperature interval $160 < T < 335$ K, with $T_M = 175$ K and $T_g = 100$ K. Because one of the donor sites in the methanol molecule is replaced by a hydrophobic group (methyl), it has one donor and one (or two) acceptor sites, and in its liquid state has both one-dimensional (chains) and two-dimensional (rings) HB networks.[19,20]

In addition to these structural anomalies, the behavior of the methanol-water solution is more complex than that found in simple molecules. The thermodynamic and transport properties are anomalous,[21] e.g., the diffusion coefficient and the excess entropy are considerably smaller and the viscosity profile becomes nonlinear when the mixing ratio is altered. This indicates that the interaction between the two liquids is strong.[22–25] There is no clear explanation for why the microscopic structure of this solution causes these surprising characteristics, although scattering experiments have revealed 3D HB networks formed by hydrophilic and hydrophobic interactions between the water and methanol molecules. Prior study of the interaction between methanol and water molecules has used a variety of experimental techniques including light,[26] X-ray,[27] and neutron scattering,[23,28] and also mass spectrometry,[29] nuclear magnetic resonance,[30] and MD simulations.[31–36]

Soft X-ray absorption spectroscopy (XAS) combined with a MD simulation study at ambient temperature (298 K) using water molar fraction X_W found three local structures around the methyl group.[27] In particular, in the methanol-rich region ($0 < X_W < 0.3$), they found a small number of water molecules around the dominant 1D/2D HB methanol cluster networks. The mixed methanol-water 3D network structures increase in the intermediate region ($0.3 < X_W < 0.7$) and make the hydrophobic interaction of the methyl group dominant due to the increase of mixed methanol-water 3D network structures. In the water-rich region ($0.7 < X_W < 0.95$), the methanol molecules are embedded separately in dominant 3D HB water networks. All of these can be seen in the in carbon K-edge XAS. The pre-edge feature in the oxygen K-edge shows an approximate linear concentration dependence indicating that the HB interaction between methanol and water is approximately the same as those of the water-water and methanol-methanol interactions.

These findings are typically understood to be caused by intermolecular clustering effects. At low methanol concentration, methanol molecules exert a slight compressive effect on the water structure. At high methanol concentration, the methyl groups are pushed together and the methanol hydroxyl groups collect around small water clusters.[23,28] Under some concentration conditions, these clusters appear to increase in size on a picosecond scale and percolate, although their structures break and rapidly reform. This suggests that the origin of the behavior of water/methanol solutions is dynamical. Depolarized Rayleigh light scattering, which gives the HB relaxation times as a function of temperature and the methanol molar fraction, indicates that the water/methanol thermodynamic anomalies are due to a complex HB dynamic behavior on the picosecond time scale.[26] In any case, this structural situation, the corresponding dynamics, and the HB strength are all strongly temperature-concentration dependent.

Traditional understandings of water-alcohol structural anomalies have assumed that the structure of normal water is significantly enhanced by hydrophobic forces that increase the local order near the methyl headgroup (an "iceberg-like" configuration).[21] At hydrophobic sites, water also loses hydrogen bonds and its enthalpy increases. To compensate for the enthalpy unbalance, the local HB arrangement of water molecules expands to form low-density water clusters with lower entropy. NMR measurements of the spin-lattice T_1 and spin-spin T_2 relaxation times of the three functional groups in water/methanol mixtures made at different water molar fractions (X_W) and temperatures ($205 < T < 295$ K) found that at all concentrations, because of the strength of the interactions, the relaxation times are shorter than those in pure water and methanol, and the result is a complex hydrogen bonding dynamics that determines the thermodynamic properties. In particular, the interplay between hydrophobicity and hydrophilicity changes with T influencing these relaxations. These results confirm that there are stable water-methanol clusters at high temperatures due to hydrophobicity, and that at low temperatures, the tetrabonded water clusters strongly influence the properties of the mixture.[30]

Here, we use techniques such as dielectric relaxation spectroscopy (DE) and NMR to study the dynamics of the water-methanol mixture. We focus on two transport parameters—relaxation time t_α and the NMR self-diffusion coefficient D—as functions of concentration X_W and temperature in the range $160 < T < 335$ K. Note that the reported relaxation time t_α measured by DE is "primary" relaxation. In our study, we use both our own data and data from the literature. In particular, we examine the evolution of the transport parameters at a fixed temperature as a function of X_W and evaluate how they differ from those in an ideal mixture in which there are no interacting molecules.

II. DATA AND DISCUSSION

Figure 1 shows an Arrhenius plot of the relaxation times t_α versus $1/T$ in pure bulk water and methanol, and of many solutions in the range $0.1 < X_W < 0.7$. As stated previously, we acquire the data from DE and NMR

Reuse of AIP Publishing content is subject to the terms: https://publishing.aip.org/authors/rights-and-permissions. Downloaded to IP: 129.74.250.206 On: Fri, 19 Feb 2016 14:05:33

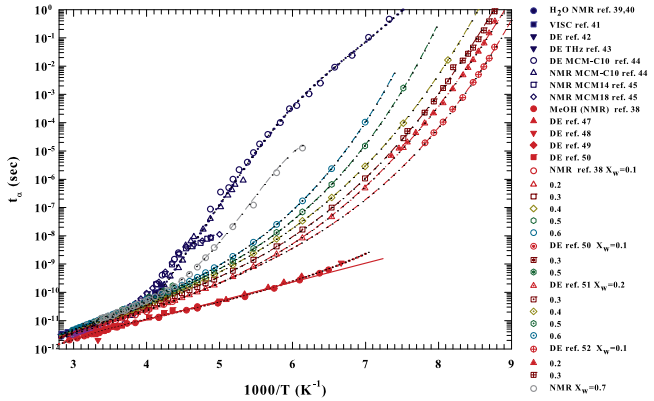

FIG. 1. The relaxation time t_α for pure water and methanol, and for many of their solutions in the range $0.1 < X_W < 0.7$ illustrated in an Arrhenius plot. A large amount of data come out from DE and NMR experiments; whereas in the case of bulk water, we also report some data extracted by the viscosity (η). In the figure, the legend indicates the literature origins of the used data (i) for bulk water: NMR,[38–40] viscosity,[41] DE relaxation[42] including the experiments in the THz region[43] and data on confined water are DE (MCM-41 C10,[44]), and NMR (MCM-41 C10,[44] MCM-41 14 and 18 Å[45]). (ii) For bulk methanol: NMR,[46] DE.[47–50] The water-methanol solution data are indicated in terms of the studied X_W: for the NMR, we have $X_W = 0.1, 0.2, 0.3, 0.4, 0.5$, and 0.6;[38] for the DE three datasets: (a) $X_W = 0.1, 0.3$, and 0.5;[50] (b) $X_W = 0.2, 0.3, 0.4, 0.5$, and 0.6;[51] (c) $X_W = 0.1, 0.2$, and 0.3.[52]

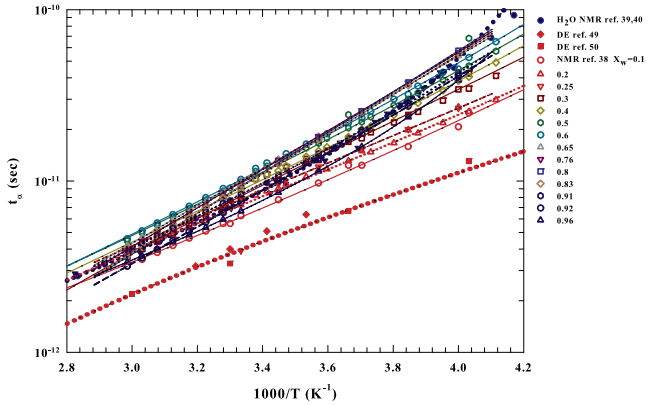

FIG. 2. This figure shows that in the high temperature region ($1000/T \lesssim 4.2$ ($T \gtrsim 238$ K)), the t_α of many different molar fractions exceeds that of water. To better illustrate such a situation, more NMR data than in Fig. 1 are reported.

experiments. In the case of bulk water, we also include viscosity η data. In this latter case, and for the NMR self-diffusion coefficient (D), we evaluate the corresponding relaxation time using the Debye-Stokes-Einstein equation and the scattering law ($t_\alpha = (Dq^2)^{-1}$).[37] The reported data are from several experiments. Figure 1 shows (i) bulk water data, including NMR,[38–40] viscosity,[41] and DE relaxation[42] including experiments in the THz region,[43] and confined water data, including DE (MCM-41 C10[44]) and NMR (MCM-41 C10[44] and MCM-41 14 and 18 Å[45]) and (ii) bulk methanol data including NMR[46] and DE.[47–50] The water-methanol solution data are indicated in terms of X_W. For NMR, we have $X_W = 0.1$, 0.2, 0.3, 0.4, 0.5, and 0.6.[38] For DE, we consider three datasets: (a) $X_W = 0.1$, 0.3, and 0.5,[50] (b) $X_W = 0.2$, 0.3, 0.4, 0.5, and 0.6,[51] and (c) $X_W = 0.1$, 0.2, and 0.3.[52] The NMR data measured at $X_W = 0.7$ are new data acquired by means of the pulsed gradient stimulated spin-echo technique (^{1}H-PGSTE), see, e.g., Ref. 38. The straight line over the pure methanol data indicates that this liquid is a strong glass former over a very large temperature range, a behavior very different from that in pure bulk water. Figure 1 shows that for all temperatures, the water relaxation time t_α^W exceeds that of methanol t_α^M. The t_α in solutions, at the different reported concentrations, shows a fragile glass-forming behavior. This is obtained using a scaling law fitting of the corresponding data (dashed curves). For water and methanol, it is obtained using simple data smoothing (dotted lines). For the scaling law, we use the ideal Mode Coupling Theory (MCT) ($t_\alpha \propto |(T - T_c)/T_c|^\gamma$), where T_c represents the "critical" MCT temperature and the exponent γ is not universal.[53] Although the MCT scaling law is used to analyze the behavior of glass forming materials, all the curves are shown as a visual aid.

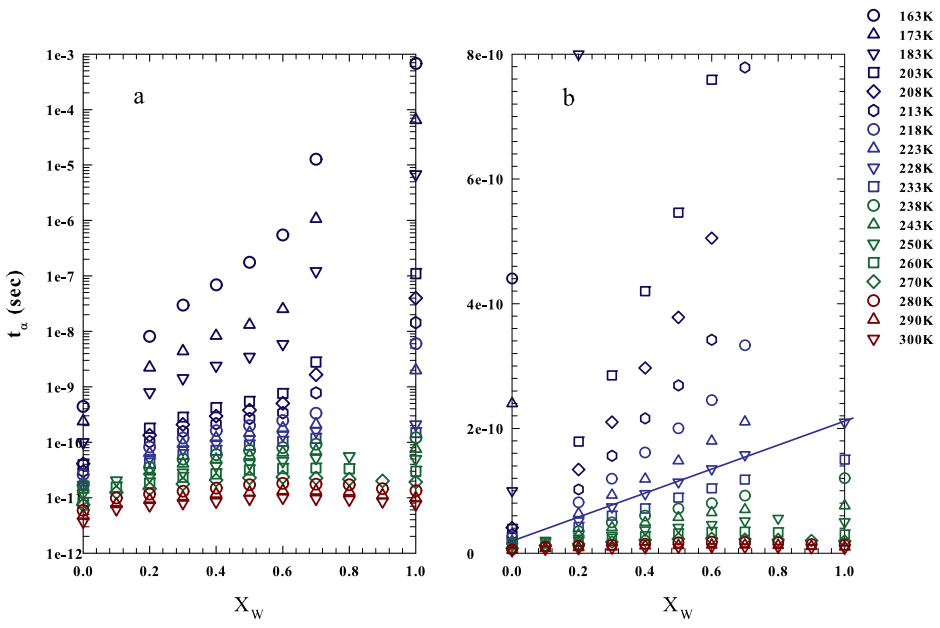

FIG. 3. The relaxation times of the water methanol mixtures, t_α, at a fixed temperature, as a function of the water molar fraction X_W. Figure 3(a) reports the data in a log-lin scale for the temperatures in the range $163 < T < 300$ K. Two different behaviors in the low and high temperature regimes are evident from these data; whereas the low-T region is characterized by a marked concavity in the t_α data, conversely in the high-T regime, the data show a maximum around $X_W \simeq 0.5$. This is more clear in the lin-lin data representation (Figure 3(b)), where a change in the data curvature, from concave to convex, takes place just near $T = 228$ K, where, within the experimental error, a nearly linear behavior (typical of an ideal mixture) can be observed.

Reuse of AIP Publishing content is subject to the terms: https://publishing.aip.org/authors/rights-and-permissions. Downloaded to IP: 129.74.250.206 On: Fri, 19 Feb 2016 14:05:33

Figure 1 shows that in the high temperature region—$1000/T \lesssim 4.2$ ($T \gtrsim 238$ K)—there is a superposition between data of many different molar fractions. Figure 2 shows the curves interpolating the pure water and methanol relaxation time data as dots. In such a way, we see that often the solution data exceed the bulk water data. In contrast, Fig. 1 shows that in the low temperature regime, the water relaxation times always exceed those of the pure methanol and the solutions. Although Fig. 2 reports more NMR data on the two components than Fig. 1, we see a change in the data-spread $(t_\alpha^W - t_\alpha^M)$ at fixed temperature. At $T \simeq 300$ K, the change is less than an order of magnitude, but at $T \simeq 150$ K, it is seven orders of magnitude, indicating a dramatic change in the solution dynamics. To further examine this, we plot the relaxation time t_α at a fixed temperature as a function of X_W. Figure 3(a) shows in a log-linear scale t_α versus X_W for temperatures $163 < T < 300$ K, revealing two different behaviors at low and high temperatures. In particular, the low-T region shows a marked concavity in the t_α data and the relaxation time data show a maximum at the high-T around $X_W \simeq 0.5$. Figure 3(b) shows a linear-linear graph in which the curvature of the data changes from concave to convex near $T = 228$ K. At that temperature, the relaxation time behavior is approximately linear within the error bars, i.e., it acts as an ideal mixture in which molecular interactions have a minimal effect on the system dynamics.

We clarify these t_α properties in water-methanol mixtures by comparing them with the linear behavior of an ideal mixture at all the studied temperatures and at different water molar fractions. To do this, we connect the measured values of t_α^W and t_α^M at the desired temperature with a straight line and subtract the solution values at the different concentrations from the straight line values at the same X_W. This produces the Δt_α values. We must mention that this procedure is the one customary used in order to evidence the interaction effects among the solution molecules with different structures and hydrophilic and hydrophobic moieties.[21–25] However, we can take profit by a simple consideration originated by a care inspection of the data behavior of Fig. 3(a); in other words, on the different behaviors shown by the relaxation time of the two opposite composition phases. That is, whereas t_α changes uniformly in the alcohol side ($X_W < 0.6$), it presents a more complex behavior at the opposite concentrations. Figure 4 shows three linear-scale graphs in which Δt_α is a function of X_W, (a) $T = 163$ K and 173 K, (b) $T = 193$ K and 203 K, and (c) $T = 208$ K, 213 K, and 218 K. Note that the Δt_α values are negative for all temperatures, but that their maximum value decreases as T increases. From 163 K to 218 K, the Δt_α values vary by four orders of magnitude. Figure 5 shows a linear plot of the results in the range $296 < T < 335$ K. Here, the Δt_α values are positive, i.e., the solution relaxation time $t_\alpha > t_\alpha^W$ value increases as the temperature decreases. Thus, the system dynamics slows, and in the low T regime inside the No Man's Land, the situation is inverted, i.e., the water–methanol interactions accelerate more than would be the case in an ideal solution. Note that Figs. 4 and 5 show that the positive excess Δt_α for all temperatures is located in the range $0.5 < X_W < 0.6$ and that the trend increases as T decreases. In contrast, in the low T regime, the negative

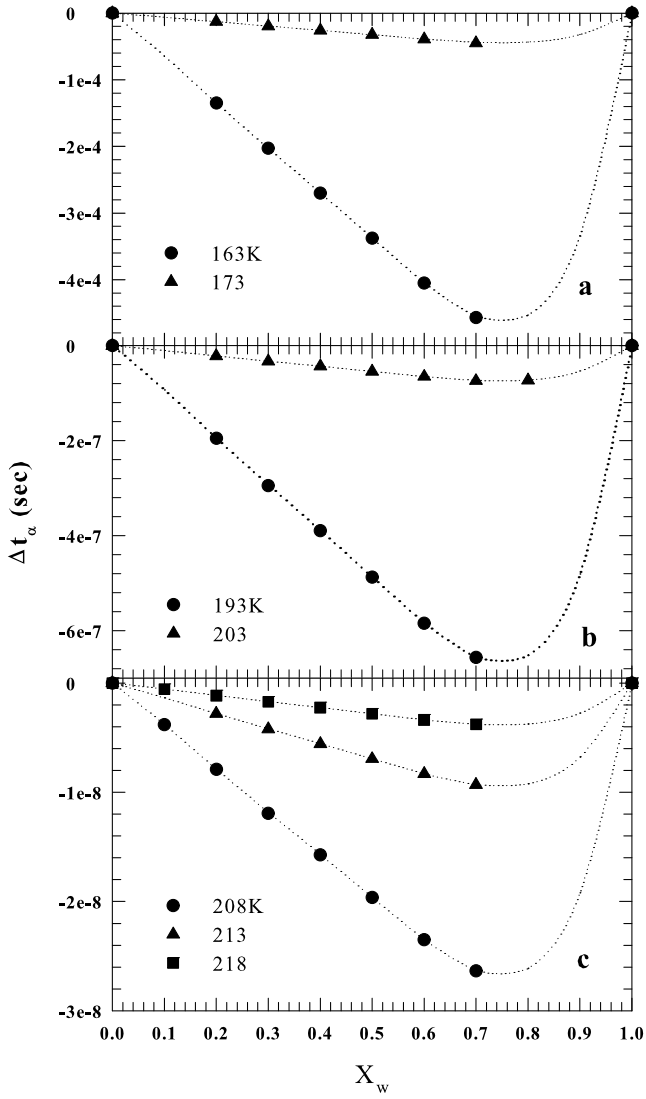

FIG. 4. The differences Δt_α between the experimental relaxation time data and those of the ideal mixture are reported in a linear scale as a function of X_W in three separate panels for $T = 163$ and 173 K (a), $T = 193$ and 203 K (b), and $T = 208$, 213, and 218 K (c). From the figure, it can be observed that the obtained Δt_α are negative for all the reported temperatures, but their maximum value decreases on increasing T; the overall variation in Δt_α is from 163 to 218 K more than four orders of magnitude.

excess is located at $X_W \simeq 0.75$. The results for $T > 223$ K are consistent with the water-methanol structural behavior results using soft X-ray absorption spectroscopy[27] at 298 K and the carbon K-edge spectra as a function of the molar concentration. The pre-edge feature in the oxygen K-edge is linear with X_W. Hence, this XAS research indicates that at room temperature, the local structure is produced by the hydrophobic interaction of the methyl group, as shown in our high-T region data. We see this also in the proton spin-lattice relaxation times T_1 measured using NMR in the range $250 < T < 300$ K, see, e.g., Ref. 38 (note that $T_1 \propto D^{54}$). In particular, the T_1 data show the same reduction seen in the t_α behavior when T is decreased (see Fig. 3).

The properties of water in the low-temperature $T < 223$ K ($\sim T_L$) regime and in the No Man's Land have been studied using MD simulations[9,55–57] and in experiments on bulk water[58] and on water in confinement.[7,59] As previously shown,

Reuse of AIP Publishing content is subject to the terms: https://publishing.aip.org/authors/rights-and-permissions. Downloaded to IP: 129.74.250.206 On: Fri, 19 Feb 2016 14:05:33

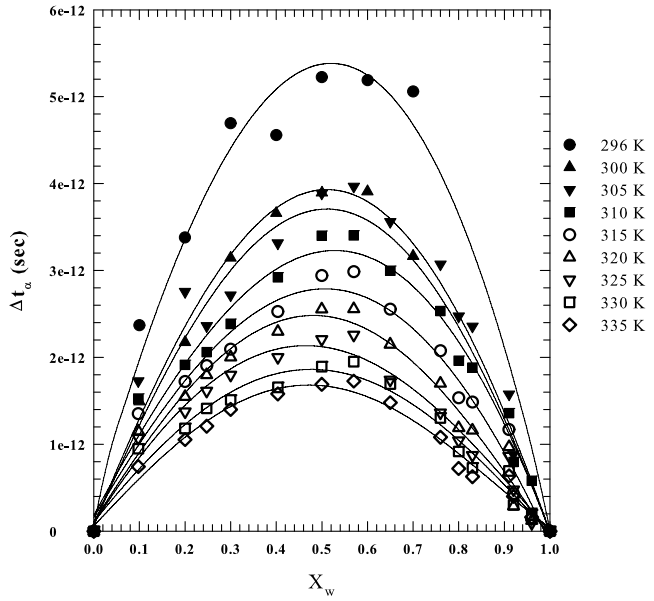

FIG. 5. A linear plot of the obtained Δt_α in the range $296 < T < 335$ K. As it can be noticed, the Δt_α values are positive and increase by decreasing temperature.

$T_L \simeq 225$ K is both the temperature of the FSDC and the Widom line temperature (T_W), which has maxima in the thermodynamic response functions in the P–T plane[3,17] (at 1 bar, $T_L = T_W$), and is the locus where the relative populations of the HDL and LDL species become the same as the temperature decreases. In particular, the regions at higher T are dominated by HDL and the deep water supercooled regime by the LDL. If we decrease T in HDL, at $T^* \simeq 320$ K, an HB network begins to form,[60] the HDL population decreases, and the LDL population increases up to T_L and becomes dominant.[7,9,57] At T^*, the bulk water compressibility has a minimum unaffected by pressure and the expansivity curves $\alpha_P(T)$ measured at different pressures cross.[60] These structural observations produced by the XAS experiment at room temperature indicate that the HB tetrahedral structure plays an important role in water-methanol solutions. When

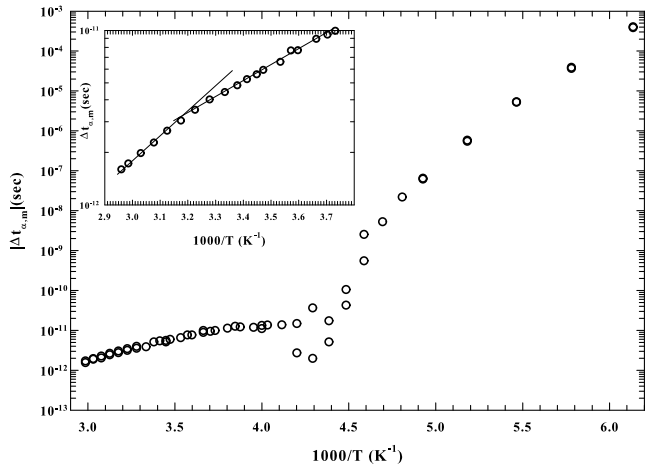

FIG. 6. The temperature behavior of the maxima variation in the relaxation times, reported in absolute units $|\Delta t_{\alpha,m}|$, illustrated in one Arrhenius plot ($|\Delta t_{\alpha,m}|$ versus $1/T$).

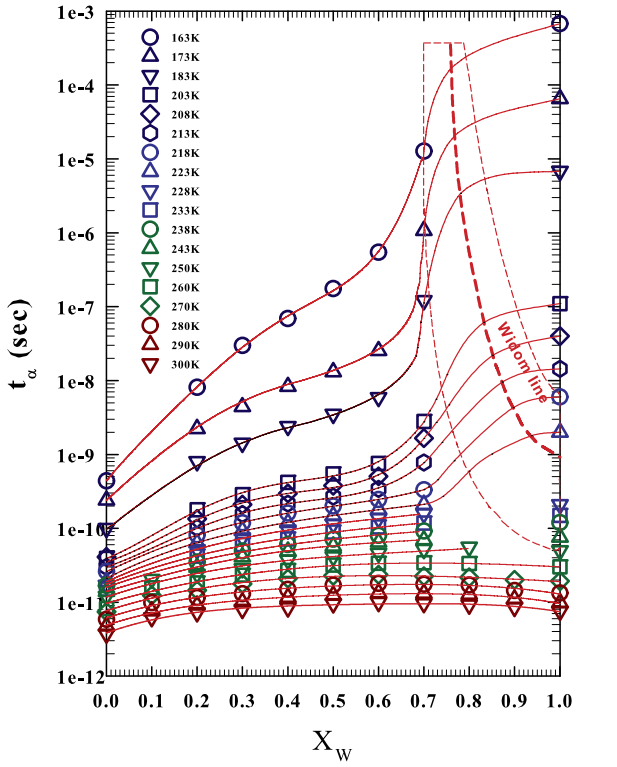

FIG. 7. The figure illustrates a new approach based on the solution relaxation time t_α from which is evidenced how the Widom line temperature may depend on the alcohol concentration.

the number of water molecules exceeds those of methanol in the concentration, i.e., $0.7 < X_W < 0.95$, the carbon K-edge indicates that the methanol molecules are separately embedded in dominant 3D HB water networks, and decreasing the temperature increases the HB relaxation time by many orders of magnitude, similar to that observed in water (see Fig. 1). This is from a side responsible for the Δt_α behavior observed in the low temperature regime, whereas from the other side, it suggests a concentration dependence of the Widom line temperature (T_W). In the high temperature regime, methyl hydrophobicity is, however, the dominant interaction.

III. CONCLUSIONS

Figure 6 shows the maximum variation in the relaxation times with respect to the ideal mixture (i.e., the minima and maxima shown in Figs. 4 and 5, respectively), reported in absolute units $|\Delta t_{\alpha,m}|$, and displayed as a function of the temperature in an Arrhenius plot ($|\Delta t_{\alpha,m}|$ versus $1/T$). This shows the dramatic change in system dynamics near T_L, where $\Delta t_{\alpha,m}$ changes from positive to negative as T is decreased. Note that the $|\Delta t_{\alpha,m}|$ data in the $4.2 < 1000/T < 4.6$ K^{-1} range are affected by large errors. Independent of the sign change in $\Delta t_{\alpha,m}$, the data show two different dynamical behaviors in the high and low temperature regimes. In the high T region, the $\Delta t_{\alpha,m}$ is positive and there is little thermal variation. The variation disappears in the $3.66 < 1000/T < 4.1$ K^{-1} range—i.e., from 273 K to 244 K—and then decreases dramatically and becomes negative. In the high temperature range, $\Delta t_{\alpha,m}$ slowly decreases by approximately one order of magnitude

Reuse of AIP Publishing content is subject to the terms: https://publishing.aip.org/authors/rights-and-permissions. Downloaded to IP: 129.74.250.206 On: Fri, 19 Feb 2016 14:05:33

as T is increased until it reaches the maximum studied temperature of 335 K (see Fig. 5). XAS and MD studies[27] indicate that in this latter T-region, the structure of the system is formed by a large HB network involving both methanol and water molecules, and that the hydrophobic interaction of the methyl groups enhances the formation process. Note that the ratio of the hydrogen donating sites between water and methanol is 1/1 and the molar ratio ≥1/1. The figure inset shows the high T-data in an enlarged scale and we see the rapidly evolving data slow to moderately evolving (the two straight lines) when T is decreased to approximately $1000/T = 3.16\ \mathrm{K}^{-1}$ ($T \simeq 318$ K). Note that this temperature is approximately coincident with T^*, i.e., the temperature above which the HB clustering ceases[60] and the water molecules are influenced solely by methyl hydrophobicity.

The $|\Delta t_{\alpha,m}|$ values in the $1000/T = 4.3\ \mathrm{K}^{-1}$ region are affected by large errors because they change from positive to negative near $T_L \simeq 225$ K (see Fig. 3). Further decreasing T causes $|\Delta t_{\alpha,m}|$ to increase by seven orders of magnitude inside the region from 220 K to 165 K where the LDL network dominates over the HDL. Note that in this supercooled region inside the No-Man's Land, these relaxation time excesses are localized for all the temperatures at approximately the same water molar fraction, $X_W \simeq 0.75$. Here, water molecules dominate over methanol molecules and produce HB structures. The system dynamics when water concentration is high and temperatures low are dominated by the LDL phase and by the increase in HB interactions. This is reflected in the pure confined water relaxation time values t_α, which for $T < T_L$ evolve from 10^{-9} s to 10^{-3} s, and the water behaves as a strong glass-forming material (see Fig. 1). Here, the methanol molecules are trapped in the LDL water network and influence the water dynamics by reducing the relaxation time of the water molecules in the HB network. This reduction is caused by changes in the hydrogen-bonding interactions imposed by the methanol hydroxyl groups (OH) linked via HBs to the LDL water network. Note also that the differences in the relaxation times between water and methanol for $T \simeq T_L$ are of approximately three orders of magnitudes and that they strongly increase as T decreases.

When $T > T_L$, the difference between t_α^{W} and t_α^{M} rapidly decreases and becomes less than one order of magnitude at ~250 K where the excess in the solution relaxation time $\Delta t_{\alpha,m}$ is positive. When the methanol and water molecules are equal in number, the relaxation time excess is due to the methyl hydrophobic component, which forces the water molecules to join a dynamical cluster of both molecular species with a relaxation time at approximately $X_W \simeq 0.5$ that is larger than the relaxation times of either liquids, t_α^{W} and t_α^{M}, considered separately. The progressive decrease of this excess by increasing T is also related to the decrease of t_α^{W} and t_α^{M}. At 298 K, these quantities are $t_\alpha^{\mathrm{W}} \simeq 8.8 \times 10^{-12}$ s and $t_\alpha^{\mathrm{M}} \simeq 4.1 \times 10^{-12}$ s.

We treat the absolute values of the relaxation time $|\Delta t_{\alpha,m}|$ in the two extreme temperature regions as an indirect measure of the bond strength and assume that both are characterized by clustering processes involving water and alcohol molecules. The difference is that the dynamic stability of the water molecules is lower at high T due to methyl hydrophobicity than that at low T, which is provided by the HBs and thus by the LDL water phase arranged in tetrahedral networks with comparatively long lifespans.

Finally, we consider that the solution dynamics changes with both temperature and concentration just by evaluating the different relaxation time behaviors in the rich water phase with respect to the opposite one, as previously stated. Hence, if our conjecture that at low T water drives the system dynamics and that the LLPT hypothesis is valid, T_L must depend on the system concentration. For this reason, we create Figure 7 by drawing lines connecting the relaxation time data points for each studied temperature (Fig. 3(a)). These lines, obtained by a simple smoothing procedure, are a guide for the eyes but illustrate well how the Widom line may depend on X_W. Figure 7 also shows that for all the temperatures with $T > 238$ K, the $t_\alpha(X_W)$ behavior is regular, vice versa in the deep supercooled regime $T < 228$ K, the relaxation time behaves in a more complex way: when the number of water molecules dominates with respect to that of the alcohol ($X_W \gtrsim 0.6$), t_α suddenly increases. However, this large increase cannot be singular (divergent) because at a certain concentration, the relaxation times must evolve slightly toward the limiting water value (see Figure 1). The water molar fraction marking the crossover between these two regimes can be reasonably related with the Widom line. In addition, the t_α of this crossover concentration increases, on decreasing T from values of the order of nano-second up to values of seconds at the lowest temperatures. Note that the crossover concentration decreases with temperature. This situation is fully consistent with the hydrophobicity effects on the HB network, being the Widom line the locus in which the LDL phase (the water HB network) dominates over the remaining HDL.

In conclusion, our experimental study has three important findings: (i) the hydrophobicity of methanol molecules dominates the dynamics of the solution when the water HB network is less developed and on the order of picoseconds or shorter (see Fig. 2); (ii) the low temperature dynamics of the solutions are strongly influenced by the structural changes in the water at its FSDC where the LDL liquid phase takes a dominant role in the deep supercooled regime and thus supports the LLPT hypothesis; (iii) in water alcohol solutions, the Widom line temperature also depends on the molar fraction: it decreases as the alcohol concentration increases.

ACKNOWLEDGMENTS

First of all, we want to thank the anonymous referees that suggested us the hypothesis that the reported time relaxation data can provide a dependence of the Widom temperature on the concentration. The Boston University work was supported by DOE Contract No. DE-AC07-05Id14517 and by NSF Grant Nos. CMMI 1125290, PHY-1505000 and CHE-1213217. Authors acknowledge the Consiglio Nazionale delle Ricerche for its support. F.M. dedicates this paper to the memory of Professor Mario P. Tosi who introduced him into the field of statistical physics.

[1]P. G. Debenedetti and H. E. Stanley, Phys. Today **56**(6), 40 (2003).
[2]O. Mishima and H. E. Stanley, Nature **396**, 329 (1998).

Reuse of AIP Publishing content is subject to the terms: https://publishing.aip.org/authors/rights-and-permissions. Downloaded to IP: 129.74.250.206 On: Fri, 19 Feb 2016 14:05:33

[3]*Liquid Polymorphism*, Advances in Chemical Physics Vol. 152, edited by H. E. Stanley (S. A. Rice, series editor) (Wiley, 2013).
[4]O. Mishima, L. D. Calvert, and E. Whalley, Nature **310**, 393 (1984).
[5]O. Mishima, L. D. Calvert, and E. Whalley, Nature **314**, 76 (1984).
[6]F. Mallamace, Proc. Natl. Acad. Sci. U. S. A. **106**, 15097–15098 (2009).
[7]F. Mallamace, M. Broccio, C. Corsaro, A. Faraone, D. Majolino, V. Venuti, L. Liu, C.-Y. Mou, and S.-H Chen, Proc. Natl. Acad. Sci. U. S. A. **104**, 424 (2007).
[8]F. Mallamace, C. Branca, M. Broccio, C. Corsaro, and S.-H. Chen, Proc. Natl. Acad. Sci. U. S. A. **104**, 18387–18391 (2007).
[9]L. Xu, F. Mallamace, Z. Yan, F. W. Starr, S. V. Buldyrev, and H. E. Stanley, Nat. Phys. **5**, 565 (2009).
[10]P. H. Poole, F. Sciortino, U. Essmann, and H. E. Stanley, Nature **360**, 324–328 (1992).
[11]H. E. Stanley *et al.*, Physica A **386**, 729 (2007).
[12]F. Mallamace, C. Corsaro, and H. E. Stanley, Proc. Natl. Acad. Sci. U. S. A. **110**, 4899–4904 (2013).
[13]A. Faraone, L. Liu, C.-Y. Mou, C.-W. Yen, and S.-H. Chen, J. Chem. Phys. **121**, 10843–10846 (2004).
[14]K. Ito, C. T. Moynihan, and C. A. Angell, Nature **398**, 492 (1999).
[15]L. Liu, S.-H. Chen, A. Faraone, C. W. Yen, and C. Y. Mou, Phys. Rev. Lett. **95**, 117802-1–117802-4 (2005).
[16]F. Mallamace, M. Broccio, C. Corsaro, A. Faraone, U. Wanderlingh, L. Liu, C. Y. Mou, and S.-H. Chen, J. Chem. Phys. **124**, 161102 (2006).
[17]L. Xu, P. Kumar, S. V. Buldirev, S.-H. Chen, P. H. Poole, F. Sciortino, and H. E. Stanley, Proc. Natl. Acad. Sci. U. S. A. **102**, 16558 (2005).
[18]S.-H. Chen, F. Mallamace, C. Y. Mou, M. Broccio, C. Corsaro, A. Faraone, and L. Liu, Proc. Natl. Acad. Sci. U. S. A. **103**, 12974–12978 (2006).
[19]A. H. Narten and A. Habenschuss, J. Chem. Phys. **80**, 3387–3391 (1984).
[20]S. Sarkar and R. N. Joarder, J. Chem. Phys. **99**, 2032–2039 (1993).
[21]H. S. Frank and M. W. Evans, J. Chem. Phys. **13**, 507–532 (1945).
[22]Z. J. Derlacki, A. Easteal, A. V. J. Edge, L. A. Woolf, and Z. Roksandic, J. Phys. Chem. **89**, 5318 (1985).
[23]A. K. Soper, L. Dougan, J. Crain, and J. L. Finney, J. Phys. Chem. B **110**, 3472 (2006).
[24]S. Z. Mikhail and W. R. Kimel, J. Chem. Eng. Data **6**, 533–537 (1961).
[25]T. W. Yergovich, G. W. Swift, and F. Kurata, J. Chem. Eng. Data **16**, 222–226 (1971).
[26]N. Micali, S. Trusso, C. Vasi, D. Blaudez, and F. Mallamace, Phys. Rev. E **54**, 1720 (1996).
[27]M. Nagasaka, K. Mochizuki, V. Leloup, and N. Kosugi, J. Phys. Chem. B **118**, 4388–4396 (2014).
[28]L. Dougan *et al.*, J. Chem. Phys. **121**, 6456 (2004); **122**, 174514 (2005).
[29]T. Takamuku, T. Yamaguchi, M. Asato, M. Matsumoto, and N. Nishi, Z. Naturforsch. A **55**, 513–525 (2000).
[30]C. Corsaro *et al.*, J. Phys. Chem. B **112**, 10449–10454 (2008).
[31]S. K. Allison, J. P Fox, R. Hargreaves, and S. P. Bates, Phys. Rev. B **71**, 024201 (2005).
[32]M. Haughney, M. Ferrario, and I. R. McDonald, J. Phys. Chem. **91**, 4934–4940 (1987).
[33]M. Ferrario, M. Haughney, I. R. McDonald, and M. L. Klein, J. Chem. Phys. **93**, 5156–5166 (1990).
[34]I. Bakó, T. Megyes, S. Bálint, T. Grósz, and V. Chihaia, Phys. Chem. Chem. Phys. **10**, 5004–5011 (2008).
[35]P. L. Silvestrelli, J. Phys. Chem. B **113**, 10728–10731 (2009).
[36]A. J. B. da Silva, F. G. B. Moreira, V. M. L. dos Santos, and R. L. Longo, Phys. Chem. Chem. Phys. **13**, 593–603 (2011).
[37]B. J. Berne and R. Pecora, *Dynamic Light Scattering with Applications to Chemistry Biology and Physics* (John Wiley and Sons, Inc., New York, 1976).
[38]C. Corsaro, R. Maisano, D. Mallamace, and G. Dugo, Physica A **392**, 596–601 (2013).
[39]W. S. Price, I. Hiroyudi, and Y. Arata, J. Phys. Chem. A **103**, 448 (1999).
[40]J. H. Simpson and H. Y. Carr, Phys. Rev. **111**, 1201 (1958).
[41]C. H. Cho, J. Urquidi, S. Singh, and G. Wilse Robinson, J. Phys. Chem. B **103**, 1991–1994 (1999).
[42]D. Bertolini, M. Cassettari, and G. Salvetti, J. Chem. Phys. **76**, 3285 (1982).
[43]C. Ronne, P. O. Åatyarnd, and S. R. Keiding, Phys. Rev. Lett. **82**, 2888 (1999).
[44]M. Sattig and M. Vogel, J. Phys. Chem. Lett. **5**, 174–178 (2014).
[45]F. Mallamace, C. Branca, C. Corsaro, N. Leone, J. Spooren, H. E. Stanley, and S.-H. Chen, J. Phys. Chem. B **114**, 1870–1878 (2010).
[46]N. Karger, T. Vardag, and H.-D. Lüdemann, J. Chem. Phys. **93**, 3437 (1990).
[47]D. J. Denney and R. H. Cole, J. Chem. Phys. **25**, 1767 (1955).
[48]H. Mandal, D. G. Frood, M. A. Saleh, B. K. Morgan, and S. Walker, Chem. Phys. **134**, 441–451 (1989).
[49]B. P. Jordan, R. J. Sheppardt, and S. Szwarnowski, J. Phys. D: Appl. Phys. **11**, 695 (1978).
[50]D. Bertolini, M. Cassettari, and G. Salvetti, J. Chem. Phys. **78**, 365 (1983).
[51]G. A. Noyel, L. J. Jorat, O. Derriche, and J. R. Huck, IEEE Trans. Electr. Insul. **27**, 1136 (1992).
[52]M. Sun, L.-M. Wang, Y. Tian, R. Liu, K. L. Ngai, and C. Tan, J. Phys. Chem. B **115**, 8242–8248 (2011).
[53]W. Götze and L. Sjögren, Rep. Prog. Phys. **55**, 241–376 (1992).
[54]T. DeFries and J. Jonas, J. Chem. Phys. **66**, 896 (1977).
[55]V. Holten *et al.*, J. Chem. Phys. **140**, 104502 (2014).
[56]L. G. M. Pettersson and A. Nilsson, J. Non-Cryst. Solids **407**, 399–417 (2015); J. Chem. Phys. **134**, 214506 (2011).
[57]K. T. Wikfeldt, A. Nilsson, and L. G. M. Pettersson, Phys. Chem. Chem. Phys. **13**, 19918–19924 (2011).
[58]J. A. Sellberg *et al.*, J. Chem. Phys. **142**, 044505 (2015); Nature **510**, 381–384 (2014).
[59]F. Mallamace *et al.*, "Transport and dynamics in supercooled confined water," in *Liquid Polymorphism*, edited by H. E. Stanley and S. A. Rice, Book Series: Advances in Chemical Physics (Wiley, 2013), Vol. 152, pp. 203-262.
[60]F. Mallamace, C. Corsaro, and H. E. Stanley, Sci. Rep. **2**, 993 (2012).

Reuse of AIP Publishing content is subject to the terms: https://publishing.aip.org/authors/rights-and-permissions. Downloaded to IP: 129.74.250.206 On: Fri, 19 Feb 2016 14:05:33